Anomalous *I–V* curve for mono-atomic carbon chains

2010 New J. Phys. 12 103017

(http://iopscience.iop.org/1367-2630/12/10/103017)

New Journal of Physics
The open-access journal for physics

Anomalous *I–V* curve for mono-atomic carbon chains

Bo Song[1,3], **Stefano Sanvito**[2] **and Haiping Fang**[1,3]

[1] Shanghai Institute of Applied Physics, Chinese Academy of Sciences, PO Box 800-204, Shanghai 201800, People's Republic of China
[2] School of Physics and CRANN, Trinity College, Dublin 2, Ireland
E-mail: bosong@sinap.ac.cn and fanghaiping@sinap.ac.cn

New Journal of Physics **12** (2010) 103017 (9pp)
Received 16 March 2010
Published 13 October 2010
Online at http://www.njp.org/
doi:10.1088/1367-2630/12/10/103017

Abstract. The electronic transport properties of mono-atomic carbon chains were studied theoretically using a combination of density functional theory and the non-equilibrium Green's functions method. The *I–V* curves for the chains composed of an even number of atoms and attached to gold electrodes through sulfur exhibit two plateaus where the current becomes bias independent. In contrast, when the number of carbon atoms in the chain is odd, the electric current simply increases monotonically with bias. This peculiar behavior is attributed to dimerization of the chains, directly resulting from their one-dimensional nature. The finding is expected to be helpful in designing molecular devices, such as carbon-chain-based transistors and sensors, for nanoscale and biological applications.

S Online supplementary data available from stacks.iop.org/NJP/12/103017/mmedia

Carbon-based nanostructures spanning different dimensionalities, going from two-dimensional (2D) graphene, to quasi-1D nanotubes, to quasi-zero-dimensional fullerenes, have already shown their potential for the case of a broad range of applications. These include molecular devices, fuel cells and structural/functional composites for bio- and nano-technology. As such they have inspired extensive studies, both experimental and theoretical [1]–[4]. Recently, a new kind of nanostructure, named mono-atomic carbon chains (MACCs), was experimentally produced by pulling out C atoms row by row from graphene [5]. In contrast with the above-mentioned nanostructures, MACCs have truly 1D features since their radius is minimal for carbon and each C atom neighbors only two other C atoms. Consequently, due to their small size,

[3] Authors to whom any correspondence should be addressed.

MACCs can easily enter biological cells and other macromolecules, and they exhibit significant quantum effects. It is thus reasonable to expect that they will open entirely new perspectives for nanoscale and biological applications and trigger many new investigations.

The electronic transport properties of a nanostructure are usually at the heart of the nanostructure's own functionality [6], since most of the possible applications consist in manipulating the electron charge. Therefore, it is interesting to investigate the electrical conductance of MACCs. Over the last few years, a number of studies have addressed this problem [7]–[16], starting from the seminal work of Guo and coworkers [7]–[11], who designed a method for calculating quantum transport in molecular junctions, and investigated various devices made either from a single atom [7] or from a small nanostructure [8]–[10]. Later, Lang and Avouris [12, 13] investigated the properties of MACCs in the limit of low voltage, and concluded that the zero-bias conductance of MACCs varies in an oscillatory manner with the number of carbon atoms in the chain. In particular, they found that the resistance of odd-numbered (ON) chains is always lower than that of the even-numbered (EN) ones [12, 13]. Subsequently, Larade *et al* [14] extended such an investigation to finite bias and presented a similar result for MACCs directly in contact with Al nanowires, for which they also reported the presence of a negative differential conductance under particular bonding conditions to the electrodes. These effects were attributed to charge transfer, resulting in a different pinning of the electrodes' Fermi level (E_F) to the chain molecular orbitals for chains with different numbers of atoms (note, however, that in this case the negative differential conductance is likely to have originated from the 1D nature of the electrodes themselves). Finally, Crljen and Baranovic [15] reported that the conductance of polyyne-formed MACCs is about one order of magnitude larger than that of other conjugated oligomers; this difference is again due to the particular line-up of the molecular levels to E_F in the two cases.

In this paper, the electronic transport properties of MACCs under bias voltage are investigated by using fully quantitative *ab initio* density functional theory (DFT) combined with the non-equilibrium Green's function method (NEGF). We find that, within a bias range of 2.0 V, the electronic current of EN chains exhibits remarkably different behavior from that of ON chains. In fact for the EN chains, there are two plateaus in the I–V curve where the current hardly varies with applied bias. In contrast, the electric current rises monotonically for ON chains. As a consequence, EN chains conduct more at low bias, while ON chains have larger electronic current at high bias, so that the two I–Vs cross over. We found that chain dimerization, directly resulting from its own 1D nature through Peierls' distortion [17], is the main reason for this peculiar electrical response. Furthermore, we also consider the situation when a molecular ring composed of six C atoms is inserted into the MACCs and find that the electronic current is, in general, greatly reduced. Such an acute sensitivity of the transport properties to the atomic details of the chain and its possible perturbation makes MACCs a promising nanostructure for logic and sensors [18].

Figure 1 illustrates several MACC-based molecular junctions in which a single MACC is connected via two S atoms to the hollow site of Au(111) electrodes. The experimental lattice constant of gold, $a = 4.078$ Å, is used for the electrodes [19], which are periodic and defined by a supercell containing ten Au atoms. The unit cell for the scattering region (the junction), i.e. the region for which the electrostatic potential is calculated self-consistently, includes the MACC, two sulfur atoms and part of the electrodes (see figure 1). Overall, this has the chemical composition $Au_{74}S_2C_n$, with n being the number of carbon atoms of the MACC, and comprises four Au monolayers on both sides, which are enough to ensure appropriate electron screening.

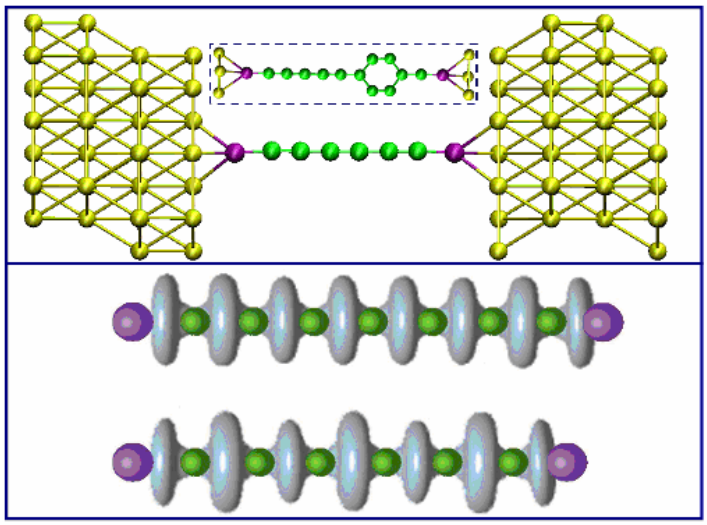

Figure 1. Upper panel: atomic conformation of the molecular junction investigated, where a MACC (green) is connected to two Au(111) electrodes (yellow) via sulfur atoms (purple). In the inset, we show the atomic conformation of the same MACC where a six-atom carbon ring is inserted into the chain. Lower panel: isosurface of the difference $\rho'(\vec{r})$ (light blue cloud) between the electron density of the MACC and that of free C atoms placed at the same positions. The upper chain contains seven atoms and the lower one only six. Note, in the case of the six-atom chain, the alternating charge accumulation and depletion resulting from Peierls' distortion.

The device geometry is optimized with DFT as implemented in the SIESTA package [20, 21]. We employ the generalized gradient approximation (GGA) in the Perdew–Burke–Ernzerhof (PBE) form for the exchange correlations functional [22]. The Troullier–Martins pseudopotentials are used to represent the ion cores, while only the valence orbitals are treated self-consistently, that is, 2s2p for carbon, 3s3p for sulfur and 5d6s for gold. Our basis set consists of double ζ orbitals plus the associated polarization functions [20, 21]. The charge density and potentials are computed on a real-space grid with an equivalent mesh cut-off energy of 350 Ryd. The force tolerance for the relaxation is set to 0.05 eV Å^{-1} and the relaxation is performed for the entire transport cell.

In general, we find that after relaxation all the MACCs remain straight [23], i.e. the C atoms align perfectly. The ON chains exhibit the geometry of cumulene with a uniform C–C bond length of 1.297 ± 0.006 Å, whereas the C–S bond length is optimized to 1.643 ± 0.003 Å. In contrast, for the EN chains, we find the geometrical conformation of polyyne with alternating short and long bonds of 1.276 ± 0.001 and 1.329 ± 0.002 Å, respectively. In this case, the C–S bond length is found to be 1.612 ± 0.003 Å. This means that only EN chains undergo dimerization.

In order to understand the effects of such a distortion over the electronic structure, we calculate the electron density difference, $\rho'(\vec{r}) = \rho(\vec{r}) - \rho_{\text{atoms}}(\vec{r})$, between the self-consistently calculated electron density of the atom chain, $\rho(\vec{r})$, and that of free C atoms placed at the same positions, $\rho_{\text{atoms}}(\vec{r})$. This density difference describes how uneven is the distribution of valence electrons between the carbon atoms in the MACCs. As shown in the upper inset of figure 1,

electrons are distributed uniformly over all C–C bonds for the ON chains, meaning that there is only a single electron-hopping probability between nearest-neighbor carbons [24]. In contrast, for EN chains, it is interesting to observe that the electron density across the short bonds is larger than that across the long ones, demonstrating an electron redistribution [15]. This leads to alternating large and small electron-hopping probabilities along the chain.

Such a chain dimerization is expected on the basis of the elementary theory of Peierl's instability [17]. In fact the parental infinite C chain is a 1D object with the Fermi level cutting across the doubly degenerate π-band. As such, the Fermi wavevector is approximately in the middle of the 1D Brillouin zone, so that the opening of an energy gap leading to a reduction of the total electronic energy requires the doubling of the unit cell, i.e. the chain dimerization. Such a mechanism is preserved for finite EN chains, but it is not for the ON ones since it is too energetically expensive to leave an unpaired C atom.

Next we investigate the electronic transport through MACC-based devices by using previously optimized atomic conformations and for bias voltages, V_{bias}, in the interval 0.0–2.0 V. Our calculations are based on DFT and NEGF method (NEGF–DFT) as implemented in SMEAGOL code [25]–[27]. An electronic temperature of 300 K is applied throughout the calculation. In order to reduce the computational overheads and make the calculations more tractable, a single ζ is used as the basis set for Au, whereas a double ζ basis is adopted for the orbitals of the other species (C and S). The use of a reduced basis for the electrodes is common practice and is well justified and documented in the literature [28, 29]. In calculating the charge density, the complex part of the integral of Green's function is computed by using 400 energy points on the imaginary semicircle, 50 points along the line parallel to the real axis and 20 poles. In addition, 1000 integration points are taken for the integral over the real energies necessary at finite bias. All the calculations are performed with periodic boundary conditions over the plane perpendicular to the direction of transport by sampling 100 k-points in the 2D Brillouin zone.

The most remarkable result of our calculations is that there are two clear plateaus in the I–V curves of the EN chains, located respectively at about $V_1 \approx 1.1$ V and $V_2 \approx 1.7$ V, where the current changes little with bias (figure 2). In contrast, for ON chains, no plateau is observed and the electric current monotonically increases across the entire bias range. This different behavior thus produces a cross-over between the I–Vs of chains with different parity. In fact, for $V_{\text{bias}} < V_1$, the electric currents of EN chains are larger than those of ON chains. However, because of the plateau at V_1, when $V_{\text{bias}} > V_1$ the electronic currents becomes larger for the odd MACCs. Our observation contrasts with the results reported in [14], where the electron current of EN chains remains always smaller than that of ON ones (here it must be noted that the bias range in [14] is actually smaller than the one considered here). Notably the chains used for the calculations of [14] were not geometrically optimized so that the C–C distance is constant regardless of the number of C atoms in the chain. Thus, we believe that Peierls' distortion is one of the reasons for the disagreement between the two calculations (in addition to the different bonding structures, the different electrode materials and the fact that in [14] the electrodes were effectively 1D objects).

Figure 3 shows the zero-bias transmission spectra $T(E - E_{\text{F}})$ as a function of energy, E, for various MACCs. We recall here that the integral of the bias-dependent transmission spectrum is proportional to the current, so that $T(E - E_{\text{F}})$ at zero bias gives information about the conduction in the linear response limit. We find that in both the energy intervals A1 ($-1.5\,\text{eV} < E - E_{\text{F}} < -0.8\,\text{eV}$) and A2 ($0.2\,\text{eV} < E - E_{\text{F}} < 1.1\,\text{eV}$) the transmission spectra of ON chains are generally greater than those of EN chains. In particular, throughout most of

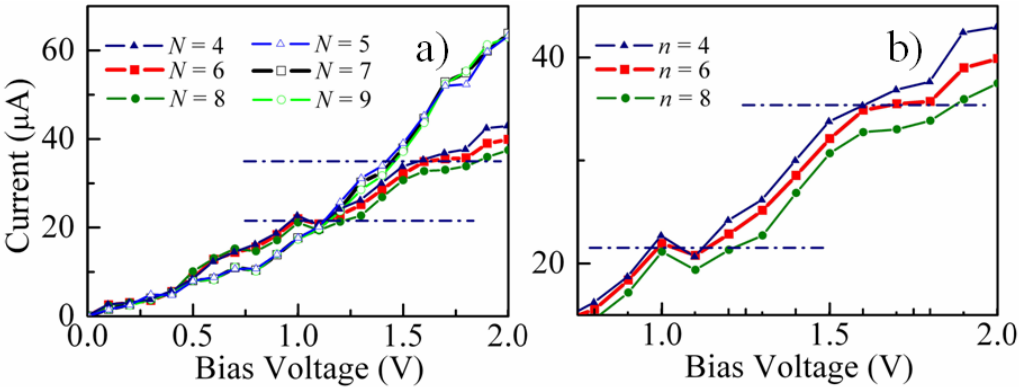

Figure 2. (a) I–V curves for MACCs with different numbers, n, of carbon atoms: $n = 4$ (-▲-), 5 (-Δ-), 6 (-■-), 7 (-□-), 8 (-●-) and 9 (-○-). The horizontal dashed-dotted lines are only a guide to the eyes and indicate the two current plateaus appearing for the EN chains. Note that the I–V curves for all the ON chains are so similar that they are almost indistinguishable. (b) Zoom of the I–V of EN chains.

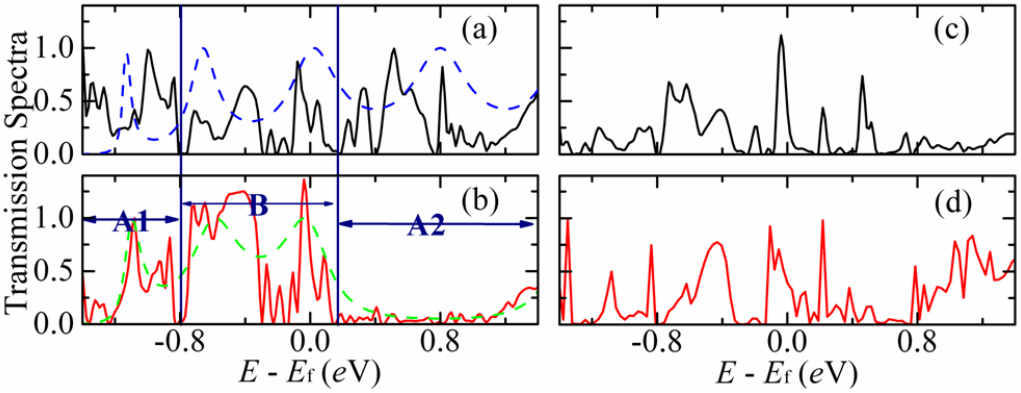

Figure 3. Transmission spectra for various MACC-based molecular junctions. (a, b) The red and black curves denote the transmission function of MACCs featuring six and seven C atoms, respectively. The green (blue) dashed line indicates the results for the six-site (seven-site) 1D chain model. (c, d) Transmission functions corresponding, respectively, to six-carbon (red) or seven-carbon (black) chains intercalating a six-carbon ring. Their geometry is displayed in the lower inset of figure 1.

region A2, the transmission of EN chains is at most 0.1, whereas that of ON chains is usually much larger. Our results indicate that, in those two regions, the molecular orbitals available for resonant tunneling are more numerous for the ON chains than for EN ones. However, in region B ($-0.8\,\text{eV} < E - E_\text{F} < 0.2\,\text{eV}$), the situation is reversed, i.e. the transmission of EN chains is generally larger than that of odd chains. If one recalls the fact that, as the bias is applied, the first spectral region to contribute to the current is that closer to the electrodes' E_F, i.e. region B, it becomes clear that the electron current at low bias will be greater for EN chains. Likewise, when V_bias becomes large enough that regions A1 and A2 of the spectra start contributing significantly to the current, the crossover happens, and the ON chains become more conductive than the EN ones.

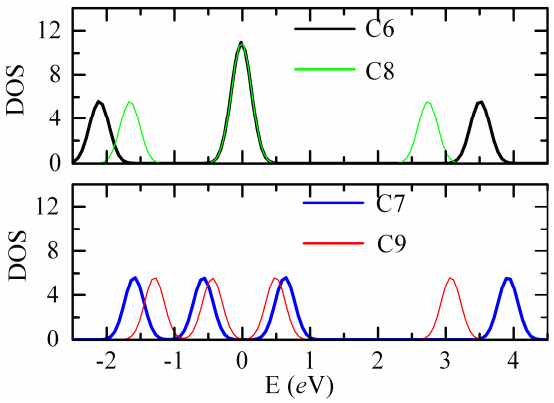

Figure 4. DOS for MACC including an even (upper panel) or an odd (lower panel) number of C atoms with 0.2 eV peak width for broadening. In this figure, $E = 0$ eV corresponds to the molecule's neutrality point, i.e. indicates the position of the HOMO.

The attribution of the different transmission features to the different molecular level distributions in the two cases is confirmed in figure 4, where we present the DFT calculated density of states (DOS) for different chains isolated from the molecular junctions without changing the bond lengths. We note that the highest occupied molecular orbital (HOMO) of the EN chains (C_6 and C_8) is a half-filled doubly degenerate state well separated from any other energy level. In contrast for the ON chains (C_7 and C_9) there are three closely spaced orbitals around $E = 0$ eV (the molecule neutrality point). This means that for EN chains only the HOMO contribute to the transmission at moderate biases, while for the ON ones the transmission can distribute over several molecular orbitals. As a consequence, the energy window over which the transmission coefficient is not small is larger for ON chains than for EN ones. Such a molecular orbital distribution maps nicely on our calculated $T(E)$, which shows large transmission only in region B for EN chains and an equally large transmission over B, A1 and A2 for ON chains.

In order to better understand the features of the various transmission spectra, we construct a simple one-dimensional nearest-neighbor tight-binding model for a chain made of N sites, one orbital per site, and attached to featureless electrodes. The Hamiltonian of such a model reads

$$H_{\mathrm{CAC}} = \sum_{i=1}^{N} \varepsilon_i d_i^{\dagger} d_i + \frac{1}{2} \sum_{i \neq j}^{N} t_{i,j} (d_i^{\dagger} d_j + d_j^{\dagger} d_i),$$

$$H_{\mathrm{electrodes}} = \sum_{\alpha,k} \varepsilon_{\alpha,k} c_{\alpha,k}^{\dagger} c_{\alpha,k},$$

$$H_{\mathrm{electrode\text{-}CAC}} = \sum_{\alpha=\mathrm{L},k} V_{1,k} (d_1^{\dagger} c_{\alpha,k} + \mathrm{h.c.}) + \sum_{\alpha=\mathrm{R},k} V_{N,k} (d_N^{\dagger} c_{\alpha,k} + \mathrm{h.c.}),$$

where H_{CAC} describes the N-atom carbon chain, with $d_i^{\dagger}$ and d_i denoting, respectively, the electronic creation and annihilation operators at site i (the chain extends from $i = 1$ to $i = N$). $t_{i,j}$ is the electron hopping parameter between sites i and j and ε_i is the on-site energy. $H_{\mathrm{electrodes}}$ and $H_{\mathrm{electrodes\text{-}CAC}}$ describe the interaction within the electrodes and between the electrodes and the chain, respectively (the S atoms are not explicitly included in the model). Here $c_{\alpha,k}$ is the annihilation operator for an electron in the electrode α with wavevector k and $\varepsilon_{\alpha,k}$ is the band

energy of the αth electrode. Finally, $V_{i,k}$ ($V_{N,k}$) is the hopping integral between a band electron in the electrodes with wavevector k and the site $i\,(N)$ of the chain.

By means of the equation of motion technique [30]–[33], we calculate the retarded/advanced (r/a) Green functions of the chain in the presence of the electrodes, namely $G^{\mathrm{r/a}}(E) = (E - H_{\mathrm{CNW}} - \Sigma^{\mathrm{r/a}})^{-1}$. Here $\Sigma^{\mathrm{r/a}} = \Sigma_{\mathrm{L}}^{\mathrm{r/a}} + \Sigma_{\mathrm{R}}^{\mathrm{r/a}}$ is the electrodes' self-energy ($\alpha = \mathrm{L}$, R), $\Sigma_{\mathrm{L}i,j}^{\mathrm{r/a}} = -\mathrm{i}\Gamma_{\mathrm{L}}\delta_{1,i}\delta_{1,j}/2$ and $\Sigma_{\mathrm{R};i,j}^{\mathrm{r/a}} = -^{\mathrm{i}}\Gamma_{\mathrm{L}}\delta_{N,i}\delta_{N,j}/2$. Γ_α denotes the level-broadening function for the electrode α, i.e. the electrodes are assumed to have a constant DOS and not to induce a level shift but only a level broadening in the chain (the real part of the self-energy vanishes). The transmission spectra can be easily calculated by using the Fisher–Lee relation $T(E) = \mathrm{Tr}\{\tilde{\Gamma}_{\mathrm{L}} G^{\mathrm{r}} \tilde{\Gamma}_{\mathrm{R}} G^{\mathrm{a}}\}$, with $\tilde{\Gamma}_\alpha = \mathrm{i}(\Sigma_\alpha^{\mathrm{r}} - \Sigma_\alpha^{\mathrm{a}})$.

In these model calculations, we always take $\varepsilon_i = 0.8\,\mathrm{eV}$ and $\Gamma_\alpha = 0.8\,\mathrm{eV}$. Furthermore, when $N = 7$, $t_{i,j}$ is constant, $t_0 \equiv 1.05\,\mathrm{eV}$, describing the uniform electron hopping in ON chains. When $N = 6$, $t_{i,j}$ alternates the values $t_\pm = t_0 \pm \Delta$ in order to describe the chain dimerization occurring in ENCA systems. In particular, we take $\Delta = 0.25\,\mathrm{eV}$. These values of the various model parameters have been chosen in order to fit better the transmission spectra calculated with NEGF–DFT. Our results are displayed in figures 3(a) and (b) (dashed curves), where we can observe relatively good agreement between the simple model and the NEGF–DFT results (given the crudeness of the model). Importantly, we observe that in our simple model the only difference between ON and EN chains is in the electron hopping parameters chosen, i.e. our model distinguishes the two types of chains only on the basis of whether the chain is dimerized or not. This allows us to conclude that the main reason for the differences in the spectra between the EN and ON chains is the different atomic configuration. Further comparison between ON and EN chains with the help of the simple model is presented in the supplementary data (available from stacks.iop.org/NJP/12/103017/mmedia).

Here, it is noted that at room temperature, the impact of vibrations on electronic current is usually of importance. We find that this impact depends on the length of the carbon chain. For the cases above (namely, there are 4–9 carbon atoms in a chain), the vibration frequency of the carbon chain is about $2400\,\mathrm{cm}^{-1}$, which corresponds to 0.3 eV, much larger than the $k_{\mathrm{B}}T$ of about 0.03 eV at the temperature $T = 300\,\mathrm{K}$, where k_{B} is the Boltzmann constant. Thus, it hardly induces the vibration of short chains at room temperature, and the phonon effect on our results is weak.

Finally, we explore the effects of perturbing the chains by calculating the transport properties of systems where a six-atom C ring is inserted in the MACCs (see the geometries of figure 1). Also in this case the devices are relaxed first and then the transport calculations are performed over the relaxed geometries. The calculated electronic currents as a function of bias are shown in figure 5, whereas in figure 3 the corresponding zero-bias transmission coefficients are presented. In general, the presence of the six-atom carbon ring greatly reduces the electron current. This can be immediately understood by looking at $T(E)$ and noting that, when compared to the pristine MACCs, the transmission of devices including the ring are generally severely suppressed. In particular, such a suppression is strong in the region $0.0\,\mathrm{eV} < E - E_{\mathrm{F}} < 0.8\,\mathrm{eV}$ for the six-atom chain and $0.0\,\mathrm{eV} < E - E_{\mathrm{F}} < 1.4\,\mathrm{eV}$ for the seven-atom one. Although it is certainly true that an intercalated molecule produces a large perturbation, our results demonstrate the sensitivity of C chains to local modification of their electronic structure. We believe that this feature can be effectively used as the driving concept for chemical nanosensors.

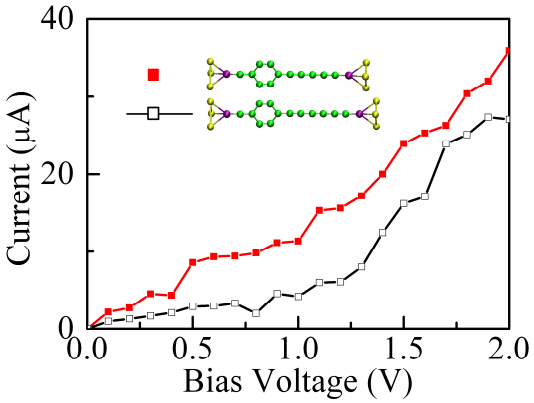

Figure 5. *I–V* curves for two devices featuring six- and seven-atom-long MACCs intercalated by a six-atom C ring (■ and □, respectively).

In conclusion, we have investigated the electronic transport properties of C mono-atomic chains in contact with Au electrodes, mainly focusing on the interplay between transport and chain geometry. We have found that EN chains conduct less than their ON counterparts at low bias, but a cross-over occurs at voltages of about 1 V. This behavior mainly originates from the presence of current plateaus in the *I–V* of EN chains, which contrasts with the monotonic current increase found for ON chains. Thus, our calculated transport features are somehow in contrast with the literature [12]–[14], with the discrepancies being attributed mainly to the different relaxed geometries utilized in our calculations. In particular, our results point to the influence of dimerization, driven by Peierls' distortion, on the EN chains' electronic structure, which reflects directly in the transmission functions of two terminal devices. We speculate that such atomic devices, so sensitive to tiny changes in their geometry, can form an intriguing materials platform for high-sensitivity sensors in physical, biological and possibly medical applications.

Acknowledgments

We acknowledge Professor David Tománek for helpful discussions. This work was supported by NNSFC (10825520), NBRPC (2007CB936000 and 2010CB934504), the Knowledge Innovation Program of the Chinese Academy of Sciences, Shanghai Leading Academic Discipline Project (B111) and the Shanghai Supercomputer Center of China. SMEAGOL code (SS) is supported by the Science Foundation of Ireland.

References

[1] Geim A K and Novoselov K S 2007 The rise of graphene *Nat. Mater.* **6** 183–91
[2] Iijima S 1991 Helical microtubules of graphitic carbon *Nature* **354** 56–8
[3] Xiang J, Lu W, Hu Y, Wu Y, Yan H and Lieber C M 2006 Ge/Si nanowire heterostructures as high-performance field-effect transistors *Nature* **441** 489–93
[4] Kroto H W, Heath J R, O'Brien S C, Curl R F and Smalley R E 1985 C60: Buckminsterfullerene *Nature* **318** 162–3
[5] Jin C, Lan H, Peng L, Suenaga K and Iijima S 2009 Deriving carbon atomic chains from graphene *Phys. Rev. Lett.* **102** 205501
[6] Nitzan A and Ratner M A 2003 Electron transport in molecular wire junctions *Science* **300** 1384–9
[7] Mozos J L, Wan C C, Taraschi G, Wang J and Guo H 1998 Transport through a single-atom junction *J. Phys.: Condens. Matter* **10** 2663–71

[8] Mozos J L, Wan C C, Taraschi G, Wang J and Guo H 1997 Quantized conductance of Si atomic wires *Phys. Rev.* B **56** 4351–4
[9] Wan C C, Mozos J L, Taraschi G, Wang J and Guo H 1997 Quantum transport through atomic wires *Appl. Phys. Lett.* **71** 419–21
[10] Taraschi G, Mozos J L, Wan C C, Guo H and Wang J 1998 Structural and transport properties of aluminum atomic wires *Phys. Rev.* B **58** 13138–45
[11] Taylor J, Guo H and Wang J 2001 *Ab initio* modeling of open systems: charge transfer, electron conduction, and molecular switching of a C_{60} device *Phys. Rev.* B **63** 121104
[12] Lang N D and Avouris Ph 1998 Oscillatory conductance of carbon-atom wires *Phys. Rev. Lett.* **81** 3515–8
[13] Lang N D and Avouris Ph 2000 Carbon-atom wires: charge-transfer doping, voltage drop, and the effect of distortions *Phys. Rev. Lett.* **84** 358–61
[14] Larade B, Taylor J, Mehrez H and Guo H 2001 Conductance, *I–V* curves, and negative differential resistance of carbon atomic wires *Phys. Rev.* B **64** 075420
[15] Crljen Z and Baranovic G 2007 Unusual conductance of polyyne-based molecular wires *Phys. Rev. Lett.* **98** 116801
[16] Tongay S, Senger R T, Dag S and Ciraci S 2004 *Ab initio* electron transport calculations of carbon based string structures *Phys. Rev. Lett.* **93** 136404
[17] Peierls R E 1955 *Quantum Theory of Solids* (London: Oxford University Press)
[18] Qian Z, Li R, Zhao X, Hou S and Sanvito S 2008 Conceptual molecular quantum phase transistor based on first-principles quantum transport calculations *Phys. Rev.* B **78** 113301
[19] Watson G M, Gibbs D, Song S, Sandy A R, Mochrie S G and Zehner D M 1995 Faceting and reconstruction of stepped Au(111) *Phys. Rev.* B **52** 12329–44
[20] Ordejón P, Artacho E and Soler J M 1996 Self-consistent order-*N* density-functional calculations for very large systems *Phys. Rev.* B **53** R10441–4
[21] Soler J M, Artacho E, Gale J D, García A, Junquera J, Ordejón P and Sánchez-Portal D 2002 The SIESTA method for *ab initio* order-*N* materials simulation *J. Phys.: Condens. Matter* **14** 2745–79
[22] Perdew J P, Burke K and Ernzerhof M 1996 Generalized gradient approximation made simple *Phys. Rev. Lett.* **77** 3865–8
[23] Okano S and Tomanek D 2007 Effect of electron and hole doping on the structure of C, Si, and S nanowires *Phys. Rev.* B **75** 195409
[24] Song B, Elstner M and Cuniberti G 2008 Anomalous conductance response of DNA wires under stretching *Nano Lett.* **8** 3217–20
[25] Rocha A R, Garcia-Suarez V, Bailey S W, Lambert C J, Ferrer J and Sanvito S 2005 Towards molecular spintronics *Nat. Mater.* **4** 335–9
[26] Rocha A R, Garcia-Suarez V, Bailey S W, Lambert C J, Ferrer J and Sanvito S 2006 Spin and molecular electronics in atomically generated orbital landscapes *Phys. Rev.* B **73** 085414
[27] Rungger I and Sanvito S 2008 Algorithm for the construction of self-energies for electronic transport calculations based on singularity elimination and singular value decomposition *Phys. Rev.* B **78** 035407
[28] Toher C and Sanvito S 2008 Effects of self-interaction corrections on the transport properties of phenyl-based molecular junctions *Phys. Rev.* B **77** 155402
[29] Toher C, Rungger I and Sanvito S 2009 Simulating STM transport in alkanes from first principles *Phys. Rev.* B **79** 205427
[30] Cuniberti G, Fagas G and Richter K (ed) 2005 *Introducing Molecular Electronics* (*Lecture Notes in Physics* vol 68) (Berlin: Springer)
[31] Meir Y and Wingreen N S 1992 Landauer formula for the current through an interacting electron region *Phys. Rev. Lett.* **68** 2512–5
[32] Song B, Ryndyk D A and Cuniberti G 2007 Molecular junctions in the Coulomb blockade regime: rectification and nesting *Phys. Rev.* B **76** 045408
[33] Haug H and Jauho A-P 1996 *Quantum Kinetics in Transport and Optics of Semiconductors* (Berlin: Springer)